

An insight into voltage-biased superconducting quantum interference devices

Chao Liu, Yi Zhang, Michael Mück, Hans-Joachim Krause, Alex I. Braginski et al.

Citation: *Appl. Phys. Lett.* **101**, 222602 (2012); doi: 10.1063/1.4768698

View online: <http://dx.doi.org/10.1063/1.4768698>

View Table of Contents: <http://apl.aip.org/resource/1/APPLAB/v101/i22>

Published by the [American Institute of Physics](#).

Additional information on *Appl. Phys. Lett.*

Journal Homepage: <http://apl.aip.org/>

Journal Information: http://apl.aip.org/about/about_the_journal

Top downloads: http://apl.aip.org/features/most_downloaded

Information for Authors: <http://apl.aip.org/authors>

ADVERTISEMENT



AIP | Applied Physics Letters

Accepting Submissions in
Biophysics and Bio-Inspired Systems

Submit Today

AIP
Publishing

An insight into voltage-biased superconducting quantum interference devices

Chao Liu,^{1,2,3,4} Yi Zhang,^{2,3,a)} Michael Mück,⁵ Hans-Joachim Krause,^{2,3} Alex I. Braginski,² Xiaoming Xie,^{1,3} Andreas Offenhäusser,^{2,3} and Mianheng Jiang^{1,3}

¹State Key Laboratory of Functional Materials for Informatics, Shanghai Institute of Microsystem and Information Technology (SIMIT), Chinese Academy of Sciences (CAS), Shanghai 200050, People's Republic of China

²Peter Grünberg Institute (PGI-8), Forschungszentrum Jülich (FZJ), D-52425 Jülich, Germany

³Joint Research Laboratory on Superconductivity and Bioelectronics, Collaboration between CAS-Shanghai, Shanghai 200050, People's Republic of China and FZJ, D-52425 Jülich, Germany

⁴Graduate University of the Chinese Academy of Sciences, Beijing 100049, China

⁵Institute of Applied Physics, University of Gießen, D-35392 Giessen, Germany

(Received 2 October 2012; accepted 8 November 2012; published online 30 November 2012)

We experimentally studied two important parameters of helium-cooled superconducting quantum interference devices (SQUIDs) in the voltage bias mode: the dynamic resistance R_d and the flux-to-current transfer coefficient $\partial i/\partial\Phi$, with different junction shunt resistors R_J . We investigated a voltage-biased SQUID using the direct readout current-to-voltage converter scheme involving an operational amplifier. At higher R_J , the flux-to-voltage conversion coefficient $\partial V/\partial\Phi$ becomes sufficiently large to effectively suppress the room-temperature amplifier's noise without any need for additional feedback circuits. The McCumber parameter limits the rise of $\partial V/\partial\Phi$. We discuss the performance of voltage-biased SQUIDs at different effective McCumber parameters. © 2012 American Institute of Physics. [<http://dx.doi.org/10.1063/1.4768698>]

In most cases, direct current superconducting quantum interference devices (dc SQUIDs) are operated in the current-biased mode. In this mode, the SQUID behavior can be well interpreted by theory, and parameters such as the McCumber parameter β_c ^{1,2} and the screening parameter β_L ³ can be determined from simulations. In voltage bias mode, it is much more difficult to simulate SQUID operation and to determine the parameters for optimum performance. The voltage-biased SQUID is connected to a voltage source, and the current flowing in the circuit is modulated by the external magnetic flux, with a period of Φ_0 , the flux quantum. We note that the SQUID intrinsic noise is independent of the selected bias mode.⁴

In contrast to a current source, which is fairly easy to realize as a SQUID exhibits a low impedance of a few tens of ohms at most, making a voltage source with an internal resistance $R_{in} \approx 0$ is very difficult. To amend this problem, two SQUID readout schemes approximating an ideal voltage source have been proposed, the two-stage SQUID⁵ and the current-to-voltage converter (CVC) using an operational amplifier.⁶ In the two-stage-SQUID scheme, the SQUID is read out by a second SQUID, thus avoiding additional noise from the room-temperature semiconductor amplifier. However, due to the necessity to bias two SQUIDs, this scheme is difficult to use and is thus not often employed in practical applications.⁴

In this paper, we statistically study two important SQUID parameters, the nonlinear dynamic resistance R_d and the current-to-flux transfer coefficient $\partial i/\partial\Phi$ of a SQUID operated in the voltage-biased mode using the CVC scheme. To obtain meaningful results, we performed the measurements

on a large number of SQUIDs (~ 100). We find that the voltage-biased SQUID offers an important technical advantage over the current-bias scheme. With an appropriately high junction shunt resistance, R_J , this SQUID can reach a low noise level even when it is directly connected to a room-temperature operational amplifier. Furthermore, we report the voltage-biased-SQUID performance at different R_J .

For our experiments, we prepared helium-cooled planar SQUID magnetometers with SQUID-loop inductance of $L_s = 350$ pH. The magnetometers consist of a parallel gradiometer SQUID with two integrated oppositely wound input coils, L_{in} , connected in series with the on-chip pickup loop L_p . The SQUIDs with a chip size of 5×5 mm² were fabricated in conventional niobium technology. Four different planar junction shunt resistors R_J of nominally 5, 10, 30, and 40 Ω were designed. The flux-to-field coefficient $\partial B/\partial\Phi$ of the magnetometers was measured to be 1.5 nT/ Φ_0 . Two planar coils, L_1 and L_2 , which can be used to implement suitable current and voltage feedbacks of SQUID bootstrap circuitry (SBC),⁷ were also integrated in the design as an option. The coil L_{FLL} was integrated on the chip for the operation in flux-locked loop mode.

The current-biased dc SQUID will convert a change in the input flux to a change in the voltage across the SQUID, while the voltage-biased SQUID will convert a flux change to a current change in the SQUID and its external circuitry. In the latter case, the two essential parameters, $R_d = \partial V/\partial i$ and the flux-to-current transfer coefficient $\partial i/\partial\Phi$, are determined by the I - V and I - Φ characteristics of the SQUID at the working point. The voltage-biased SQUID is directly connected to the inverting input of an operational amplifier, while the bias voltage is applied at its non-inverting input (see the inset of Fig. 1). The operational amplifier has two noise sources, the

^{a)}Author to whom correspondence should be addressed. Electronic mail: y.zhang@fz-juelich.de.

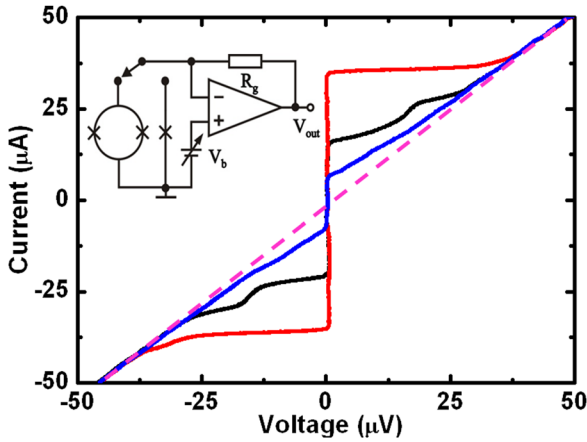


FIG. 1. Current-voltage characteristics of three junctions with different I_c . Here, the source resistances R_{in} have been taken out with data processing. Inset depicts the current-to-voltage converter scheme used in this work.

voltage noise V_n , and the current noise I_n^* , which must be taken into account. The total current noise I_n flowing from the preamplifier output is $I_n = [(V_n/R_d)^2 + I_n^{*2}]^{1/2}$, where R_d denotes the dynamic resistance of the SQUID. The equivalent flux noise of the preamplifier is $\delta\Phi_{amp} = I_n/(\partial i/\partial\Phi)$. Generally, the contribution of I_n^* is independent of R_d and can be ignored in the voltage bias mode.⁸ Consequently, the expression can be simplified to $\delta\Phi_{amp} = (V_n/R_d)/(\partial i/\partial\Phi) = V_n/(\partial V/\partial\Phi)$. The voltage-bias parameter $\partial V/\partial\Phi$ is a product of R_d and $\partial i/\partial\Phi$. In our experiments, we used the low noise operational amplifier Analog Devices 797 with a typical voltage noise of $V_n \approx 1 \text{ nV}/\sqrt{\text{Hz}}$ in the white noise range ($>100 \text{ Hz}$).

It is illustrative to first measure junctions in the CVC scheme. Figure 1 shows measured I - V characteristics of single junctions with different critical currents I_c . Each junction was shunted by the resistance $R_J = 1 \Omega$. The dashed line describes the shunted junction's normal resistance $R_N \approx R_J$. In the non-linear regime, i.e., at low voltages R_d increases with increasing I_c . The I_c values were measured to be about 6.4, 15.5, and 34 μA , which resulted in dynamic resistances $R_d \approx 1.2 \Omega$, 3 Ω , and 25 Ω , respectively.

According to theory,⁹ a critical current I_c of about $\Phi_0/2L_s$ is needed to obtain the optimum SQUID screening parameter of $\beta_L \approx 1$. We investigated the dependence of R_d and $\partial i/\partial\Phi$ upon R_J using different junction shunt resistors R_J of 5, 10, 30, and 40 Ω . Overall, 101 SQUID magnetometers were measured to obtain the averaged data illustrated in Fig. 2. The

statistical data showed that R_J increasing from 5 Ω to 40 Ω resulted in SQUID current swing I_{swing} decreasing from 4.6 μA to 2.9 μA (a), which corresponded to $\partial i/\partial\Phi$ from 14 $\mu\text{A}/\Phi_0$ to 9 $\mu\text{A}/\Phi_0$, while R_d increased from 6.5 Ω to 44 Ω (b). The product $(\partial i/\partial\Phi) \times R_d = \partial V/\partial\Phi$ increased up to about 400 $\mu\text{V}/\Phi_0$ at $R_J = 30$ to 40 Ω . High R_J leads to a large $\partial V/\partial\Phi$, thus reducing the preamplifier noise contribution $\delta\Phi_{amp}$. A large R_J is also required for a low SQUID intrinsic flux noise spectral density, which is $S_\Phi = 16k_B T L_s^2/R_J$ at the optimal $\beta_L \approx 1$, where k_B denotes the Boltzmann constant and $T = 4.2 \text{ K}$.

Deviations of the SQUID parameters from the design values due to variations in the fabrication processes cannot be avoided. In our case, the maximum-to-minimum ratios of the two parameters shown in Fig. 2 were rather large, e.g., in the case of $R_J = 30 \Omega$, the ratios were about 2 for I_{swing} and 3 for R_d . The SQUID's intrinsic noise does not depend on these two parameters directly, but $\delta\Phi_{amp}$ in direct readout electronics does. As shown below, adding an additional feedback circuitry helps to overcome the drawbacks of large parameter spreads.

Measurements of noise at different R_J values were performed in a flux-locked loop, while the SQUID magnetometer chip, whose equivalent circuit is shown in the inset of Fig. 3, was placed in a niobium tube. We used our direct readout CVC scheme with the working point selected at maximum $\partial i/\partial\Phi$ in measured I - Φ characteristics.

Figure 3 shows noise measurements of SQUIDs with different R_J : (I) 5 Ω , (II) 10 Ω , and (III) 30 Ω . The measured flux noise decreased from 17 $\mu\Phi_0/\sqrt{\text{Hz}}$ (I) to 13 $\mu\Phi_0/\sqrt{\text{Hz}}$ (II) and 4 $\mu\Phi_0/\sqrt{\text{Hz}}$ (III). The lowest value corresponds to a field resolution $\sqrt{S_B} \approx 6 \text{ fT}/\sqrt{\text{Hz}}$ in the white noise range. Clearly, $\partial V/\partial\Phi$ increases with R_J so that $\delta\Phi_{amp}$ is increasingly suppressed. We note that here the measured noise was mainly determined by the voltage noise of the room-temperature preamplifier rather than by the SQUID itself.

We then used the additional feedback circuitry, SBC,⁷ which is already integrated on our SQUID chip, to further reduce $\sqrt{S_\Phi}$. Using the SBC readout scheme, the flux noise of SQUID (II) reached about 3 $\mu\Phi_0/\sqrt{\text{Hz}}$ ($\sqrt{S_B} < 5 \text{ fT}/\sqrt{\text{Hz}}$), as shown in Fig. 3 IV. In the case of larger $R_J \geq 30 \Omega$, the noise of some SQUIDs with smaller $\partial V/\partial\Phi$ resulting from the parameter spread in fabrication was also improved to this level (data not shown here).

Generally, a junction Stewart-McCumber parameter $\beta_c \equiv 2\pi I_c R_J^2 C/\Phi_0 < 1$ is required for SQUID operation in

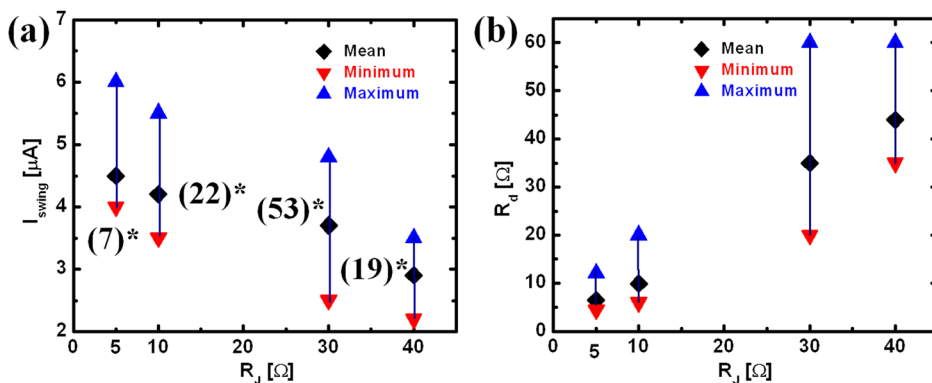


FIG. 2. Statistical data of I_{swing} and R_d of 101 voltage-biased SQUIDs as a function of R_J . (...) denotes the number of samples.

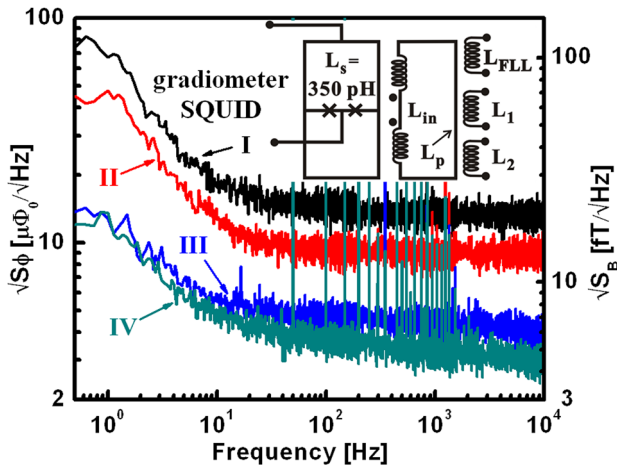


FIG. 3. Flux noise $\sqrt{S_\Phi}$ measurements (right ordinate gives the field resolution $\sqrt{S_B}$) of SQUIDs with different R_J operated in voltage bias mode using the CVC readout scheme. The inset shows the equivalent circuit of the measured magnetometers described above.

both current and voltage bias mode; here, C denotes the junction's self-capacitance. The source resistance R_{in} is parallel to R_J and shunts it in the voltage bias mode. From simulations by Warman and Blackburn,¹⁰ it is known that with decreasing ratio of source and junction resistance, R_{in}/R_J , the junction hysteresis disappears and eventually a negative dynamic resistance appears. For SQUIDs biased by a source of sufficiently small R_{in} , its shunting effect, which leads to effective $\beta_{ce} < \beta_c$, was first reported by Zhang *et al.*¹¹ At $\beta_{ce} > 1$, a negative resistance appears in SQUID characteristics, which can lead to instabilities or oscillations in the readout circuit. The enhancement of SQUIDs $\partial V/\partial \Phi$ with increasing R_J is limited by the requirement that β_{ce} remains less than one.

It is known that the SQUID I - V and V - Φ characteristics both exhibit hysteresis at $\beta_c > 1$ in current bias mode. The value of β_c can be estimated from the amount of hysteresis observed in the characteristics. Here, we report on the voltage-biased SQUID performance in the range from $\beta_{ce} < 1$

to $\beta_{ce} \gg 1$ using the I - Φ characteristic as our test signal. Figure 4 shows measured I - Φ characteristics of SQUIDs with different R_J values. In Fig. 4(a), $R_J = 10 \Omega$, the I - Φ characteristics exhibits a quasi-triangular-shaped curve without any distortion and a large current swing. Its average value is $I_{swing} = 4.2 \mu A$. In this case, $\delta\Phi_{amp}$ can be effectively reduced by using SBC, as shown in Fig. 3 IV. We infer this case corresponds to $\beta_{ce} < 1$. At higher nominal values of R_J ($R_{in} = \text{constant}$), we observe increasing distortions and oscillations in the I - Φ characteristics. In Fig. 4(b), nominal $R_J = 40 \Omega$, at the bottom of the I - Φ curve a distortion and oscillation are visible. The inferred β_{ce} is ≈ 1 . In this SQUID, the intrinsic noise is higher than that in SQUID (a); the measured data are not shown here. In Fig. 4(c), with R_J nominally also 40Ω , the oscillation appears at most parts of the I - Φ curve, and measured noise is still higher, so presumably $\beta_{ce} > 1$. In Fig. 4(d), for the case of $R_J = 200 \Omega$, a strong oscillation dominates the whole I - Φ dependence; here, we clearly have $\beta_{ce} \gg 1$.

All our voltage-biased SQUIDs with $R_J = 30 \Omega$ operated very stably and exhibited a good noise performance, even without SBC. The I - Φ traces were as in Fig. 4(a).

In conclusion, our experimental and statistical investigation has shown that the SQUID direct readout current-to-voltage converter scheme permits one to largely suppress the noise contribution of the room-temperature operational amplifier. To achieve this, the junction shunt resistance should be appropriately high, but the effective McCumber parameter less than 1. Consequently, provided that fabrication of SQUIDs with tight parameter spreads is attained, it should be possible to use the direct readout CVC scheme without any additional feedbacks and further simplify the readout. In the case of wide parameter spreads, a feedback scheme, such as the SQUID bootstrap circuit, is useful in effectively suppressing the noise contribution of the amplifier.

These results help to understand SQUIDs operated in voltage bias mode and can be used to develop very simple multi-channel SQUID systems, e.g., for biomagnetic measurements.

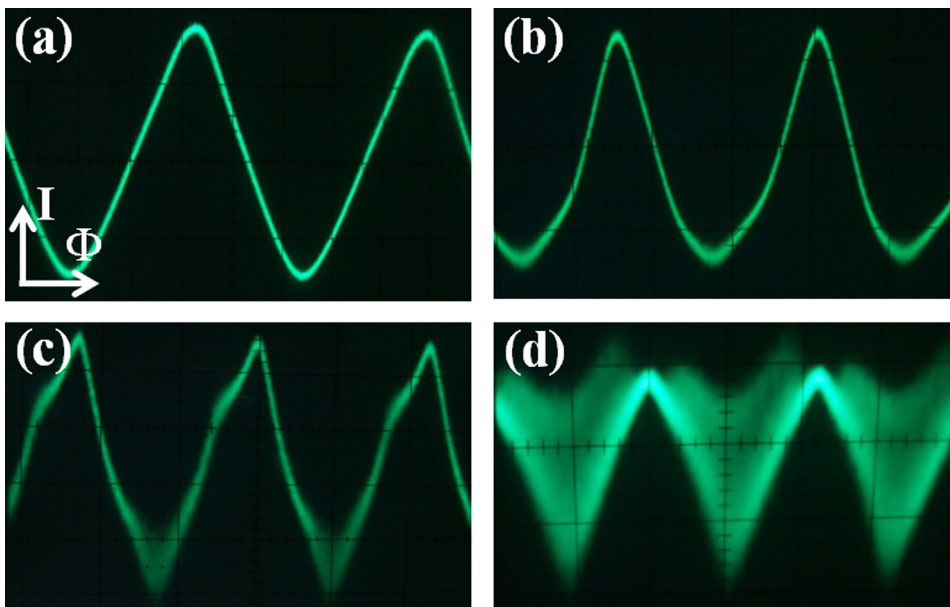


FIG. 4. I - Φ characteristics at $\beta_{ce} < 1$ (a), $\beta_{ce} \approx 1$ (b), $\beta_{ce} > 1$ (c), and $\beta_{ce} \gg 1$ (d).

The authors thank Dr. Zhen Wang, Dr. Guofeng Zhang, and Mr. Yongliang Wang for the help to measure the I - V characteristics of junctions.

- ¹W. C. Stewart, *Appl. Phys. Lett.* **12**, 277–280 (1968).
- ²D. E. McCumber, *J. Appl. Phys.* **39**, 3113–3118 (1968).
- ³J. Clarke, in *The SQUID Handbook*, edited by J. Clarke and A. I. Braginski (Wiley-VCH, Weinheim, 2004), Vol. I, pp.1–28.
- ⁴D. Drung and M. Mück, in *The SQUID Handbook*, edited by J. Clarke and A. I. Braginski (Wiley-VCH, Weinheim, 2004), Vol. I, pp.127–170.
- ⁵F. C. Wellstood, C. Urbina, and J. Clarke, *Appl. Phys. Lett.* **50**, 772 (1987).
- ⁶H. Seppä, A. Ahonen, J. Knuutila, J. Simola, and V. Vilkmann, *IEEE Trans. Magn.* **27**, 2488–2490 (1991).
- ⁷X. Xie, Y. Zhang, H. Wang, Y. Wang, M. Mück, H. Dong, H.-J. Krause, A. I. Braginski, A. Offenhäusser, and M. Jiang, *Supercond. Sci. Technol.* **23**, 065016 (2010).
- ⁸G. Zhang, Y. Zhang, H. Dong, H.-J. Krause, X. Xie, A. I. Braginski, A. Offenhäusser, and M. Jiang, *Supercond. Sci. Technol.* **24**, 065023 (2011).
- ⁹C. D. Tesche and J. Clarke, *J. Low Temp. Phys.* **29**, 301–331 (1977).
- ¹⁰J. Warman and J. A. Blackburn, *Appl. Phys. Lett.* **19**, 60 (1971).
- ¹¹Y. Zhang, C. Liu, M. Schmelz, H.-J. Krause, A. I. Braginski, R. Stolz, X. Xie, H.-G. Meyer, A. Offenhäusser, and M. Jiang, *Supercond. Sci. Technol.* **25**, 125007 (2012).